

## ORIGINAL ARTICLE

# Arginine vasopressin ameliorates spatial learning impairments in chronic cerebral hypoperfusion via V1a receptor and autophagy signaling partially

C Yang, X Zhang, J Gao, M Wang and Z Yang

Chronic cerebral hypoperfusion (CCH) is a major factor contributing to neurological disorders and cognitive decline. Autophagy activation is believed to provide both beneficial and detrimental roles during hypoxic/ischemic cellular injury. Although arginine vasopressin (AVP) has been strongly involved in many behaviors, especially in learning and memory, the effects of AVP on CCH and their molecular mechanisms remain unclear. Here, to investigate whether there was neuroprotective effects of AVP on CCH through V1a receptor (an AVP receptor) signaling, permanent bilateral carotid arteries occlusion (two vessel occlusion, 2VO) was used to establish a rat model of CCH, and hypertonic saline (5.3%) was injected intraperitoneally to induce the secretion of AVP. Results showed that hypertonic saline effectively alleviated spatial learning and memory deficit, enhanced synaptic plasticity of CA3-CA1 hippocampal synapses, upregulated *N*-methyl-D-aspartate receptor subunit 2B (NR2B) and postsynaptic density protein 95 (PSD-95) surface expressions, reduced oxidative stress and increased Nissl bodies in 2VO model rats. These phenomena were significantly decreased by V1a receptor antagonist SR49059. Interestingly, hypertonic saline also upregulated autophagy in the hippocampus of 2VO rats partly through V1a receptor. These findings imply that AVP has a beneficial role for the treatment of cognitive impairments partly through V1a receptor signaling in CCH, which is possibly related to improving synaptic plasticity by promoting NR2B and PSD-95 externalization and by enhancing autophagy.

*Translational Psychiatry* (2017) **7**, e1174; doi:10.1038/tp.2017.121; published online 18 July 2017

## INTRODUCTION

Chronic cerebral hypoperfusion (CCH) has been associated with cognitive decline in aging, Alzheimer's disease and vascular dementia.<sup>1,2</sup> Previous studies have revealed that CCH induces age-related blood-brain barrier damage, neuronal cell death, oxidative stress and impairment of spatial learning.<sup>1</sup> Till now, pharmacological and immunologic interventions in reducing cognitive impairments in patient populations suffering neurodegenerative diseases have met with limited success.<sup>3</sup> Thus, it is of great importance to seek novel therapy. The occlusion of both carotid arteries (two vessel occlusion, or 2VO) is a well-established rat model of CCH developed by De la Torre *et al.*<sup>4</sup> It was found to reduce cerebral blood flow by 21% in the cortex and by 32% in the hippocampus of middle-aged rats.<sup>5</sup> Experimental lines of evidence have demonstrated that 2VO rat model is suitable for the development of potentially neuroprotective strategies in neurodegenerative diseases.

Arginine vasopressin (AVP), a neurohypophyseal nonapeptide hormone, not only targets kidney, blood vessels, liver, platelets and anterior pituitary, but also serves as a neuromodulator in the brain.<sup>6</sup> AVP exerts its effects through three subtypes of receptors: V1a and V1b receptors are coupled to G<sub>q</sub> and phospholipase C, which increase intracellular Ca<sup>2+</sup> release, whereas the V2 receptor is coupled to G<sub>s</sub> and activates adenylate cyclase resulting in increases in levels of cyclic AMP and protein kinase A activity.<sup>6</sup> Only V1a and V1b receptor subtypes exist in the central nervous

system.<sup>7</sup> In the hippocampus, V1a receptor (V1aR) is present in the dentate gyrus as well as in the CA1, CA2 and CA3 fields.<sup>7,8</sup> On the contrary, V1b receptor is restricted to the CA2 field.<sup>9</sup> A number of studies have showed that central AVP has influence in many types of behaviors, especially learning and memory. In terms of electrophysiology, the application of vasopressin enhances synaptic transmission and induces long-term potentiation (LTP) in the CA1 region<sup>10,11</sup> and the dentate gyrus,<sup>12</sup> which is consistent with the distribution of vasopressin and vasopressin receptors in the hippocampus. In an examination of spatial learning, Egashira *N et al.*<sup>13</sup> found that V1aR knockout (KO) mice, but not V1bR-KO mice, exhibited an impairment of spatial memory compared to wild-type mice in an eight-arm radial maze. Moreover, a selective V1aR antagonist (OPC-21268) impaired spatial memory in the eight-arm radial maze in wild-type mice. These results suggest that the V1aR is required for working memory or a high level of spatial memory in a radial arm maze. However, the effects of endogenous AVP on CCH are less reported, and whether V1aR is involved in such a process remains unclear.

Autophagy is an evolutionarily conserved process of self-digestion and recycling of cellular constituents, participating in organelle turnover and bioenergetic management during starvation from yeast to mammals.<sup>14–16</sup> Studies have reported that autophagy can have both protective and injurious roles in many pathological conditions, including cerebral hypoxia-ischemia.<sup>17</sup> Autophagy has been found to be neuroprotective, as it involves in

abnormal protein and organelle degradation and prevents protein aggregation, which exhibits an astonishing number of connections to neurodegenerative diseases.<sup>15,18–21</sup> Some reports have showed that autophagy protects neurons from ischemia-induced death.<sup>22–24</sup> However, excessive autophagy destroys large proportions of the cytosol and organelles, causing cellular atrophy and apoptosis or necrotic cell death.<sup>25</sup> Other researches have demonstrated that autophagy in brain ischemia may contribute to neural damage, and the inhibition of autophagy can attenuate cerebral ischemia-associated neuronal death.<sup>26–29</sup> Thus, the survival or death contribution of autophagy in the chronic ischemic rats requires further study.

In the present study, we tested the hypothesis that whether endogenous AVP can ameliorate spatial learning and synaptic plasticity through the V1aR signaling in 2VO rats, and whether autophagy was related to these effects. Our investigation will shed new light on the relation of autophagy to endogenous AVP on 2VO rats, and might provide useful clues to relieve the damage induced by CCH, such as mild cognitive impairment, vascular dementia and Alzheimer's disease.

## MATERIALS AND METHODS

### Animal care

Specific pathogen-free adult male Wistar rats weighting 220–250 g were purchased from the Experimental Animal Center of the Chinese Academy of Medical Science, and reared in the Animal House of Medical School, Nankai University. The room temperature was kept at  $24 \pm 1$  °C, and rats were housed in groups of four in clear plastic cages under a 12-h light–dark cycle with lights on from 0800 hours. Food and water were freely available. All animal experiments were approved by the Animal Research Ethics Committee of the Nankai University and were performed in accordance with the Animal Management Rules of the Ministry of Health of the People's Republic of China. All efforts were made to minimize the animals' suffering.

### Induction of 2VO

Rats were randomly divided into four groups, sham group ( $n=8$ ), 2VO group ( $n=8$ ), 2VO + hypertonic saline (2VO + HTS) group ( $n=8$ ) and 2VO + HTS + SR49059 (2VO + HTS + SR49059) group ( $n=8$ ). The induction of 2VO rat model was described in Supplementary Materials and Methods as previously reported,<sup>30</sup> based on the fact that rats have complete circle of Willis, which can afford constant blood flow after the onset of occlusion. The time for postoperative recovery was 14 days.

### Drug application

SR49059 (Sigma-Aldrich, St Louis, MO, USA), the most potent nonpeptide competitive V1aR antagonist,<sup>31</sup> was initially dissolved in dimethyl sulphoxide at a concentration of 30 mM, and then diluted with 0.9% NaCl to 0.3 mM as a final concentration. The drug application timeline was shown in Supplementary Figure S1. Since the 15th day after 2VO surgery, the 2VO + HTS group was given 5.3% NaCl (refs 32,33) as a single intraperitoneal injection of 2% bodyweight, 1 h before the Morris water maze (MWM) or LTP every day.<sup>32,34</sup> The 2VO + HTS + SR49059 group was given  $0.3 \text{ mg kg}^{-1}$  ( $1.67 \text{ ml kg}^{-1}$ , 0.3 mM) SR49059 (refs 35,36) intravenously through the tail vein at 30 min following injection of 5.3% NaCl as described above, and the sham and 2VO groups received 0.9% NaCl as control. Water bottles were removed at the moment of first injection for all groups until 10 min before MWM and LTP.

### MWM experiment

The spatial learning and memory abilities of rats were measured by MWM (RB-100A type, Beijing, China) as previously reported.<sup>37,38</sup> Experimental details of MWM test were given in Supplementary Materials and Methods.

### *In vivo* LTP recording

The LTP recording from Schaffer collaterals to hippocampal CA1 was performed on rats after MWM experiment as previously described.<sup>39,40</sup> The specific methods of inducing and recording LTP were shown in the

Supplementary Materials and Methods. After LTP recording, and after suffering ~4 weeks from bilateral carotid artery occlusion, all rats were killed and their brains were removed for the preparation of coronal sections and hippocampal proteins. Tissue preparation details were provided in Supplementary Materials and Methods.

### Immunofluorescence

The brain coronal sections were obtained at 6  $\mu\text{m}$  and stained with antibodies against AVP, V1aR, LAMP1 and LC3. Further details were provided in Supplementary Materials and Methods.

### Subcellular fractionation of hippocampal tissues and protein extraction

For the detection of synaptic protein expressions, subcellular fractionation experiment was performed following the standard methods<sup>41</sup> and the study by Won *et al.*<sup>42</sup> with slight modifications (Supplementary Figure S2A). However, proteins extracted with RIPA lysis buffer were used for the assessment of AVP and V1aR expressions, besides autophagy and oxidative stress levels. See Supplementary Materials and Methods for details.

### Western blot assay

Protein expressions were analyzed with western blot assay. Polyvinylidene difluoride membranes (Millipore, Billerica, MA, USA) were incubated with primary antibodies including Anti-AVP, Anti-V1aR, Anti-NR2B (*N*-methyl-D-aspartate receptor subunit 2B), Anti-PSD-95 (postsynaptic density protein 95), Anti-synaptophysin (SYP), Anti-SQSTM1/p62 (p62), Anti-Becn1, Anti-LC3 and Anti- $\beta$ -actin. Further details were described in the Supplementary Materials and Methods.

### Measurement of oxidative parameters in the hippocampus

The levels of total malondialdehyde (MDA), superoxide dismutase and catalase activities in the hippocampus were evaluated by the assay kits (Beyotime Biotechnology, Shanghai, China), according to the manufacturer's directions.

### Statistical analysis

The number of animals used for each test is reported in figure legends. The sample sizes were determined using PASS 11 software (NCSS, Kaysville, UT, USA). We hypothesized the means and assumed an equal s.d. for each group based on a pre-specified effect size and previous studies. With  $\alpha=0.05$  and a power of 99%, we needed minimum three animals per group in MWM, LTP and western blot assays. Double blinding method was used for group assignment and outcome assessment. All data were analyzed with SPSS 22 software (IBM, Armonk, NY, USA) and presented as mean  $\pm$  s.e.m. Statistical significance was determined as indicated by applying the Mann–Whitney *U*-test (non-normal distribution), one-way analysis of variance (ANOVA) and two-way repeated measures ANOVA with least significant difference (LSD) (for equal variances) or Dunnett's T3 (for unequal variances) *post hoc* test (normal distribution). Differences were considered significant at  $P < 0.05$ . All experiments were repeated at least three times independently.

## RESULTS

### The effects of HTS and SR49059 on AVP and V1aR expression levels

To determine whether the concentration of AVP in the hippocampus would increase by HTS, and whether SR49059 would work, we measured the levels of AVP and V1aR in the hippocampus by western blot assay and immunofluorescence staining. It can be seen that AVP and V1aR expressions were significantly decreased in the 2VO group compared with those of the sham group (Figures 1a and b, AVP,  $P < 0.05$ ; Figures 1a and c, V1aR,  $P < 0.01$ ), and HTS was able to increase both levels of AVP and V1aR statistically in 2VO rats (Figures 1a and b, AVP,  $P < 0.01$ ; Figures 1a and c, V1aR,  $P < 0.01$ ). When administered with SR49059, the level of V1aR, but not AVP, was decreased effectively (Figures 1a and c,  $P < 0.01$  versus 2VO + HTS). As shown in Figures 1d and e, AVP and V1aR were stained with green

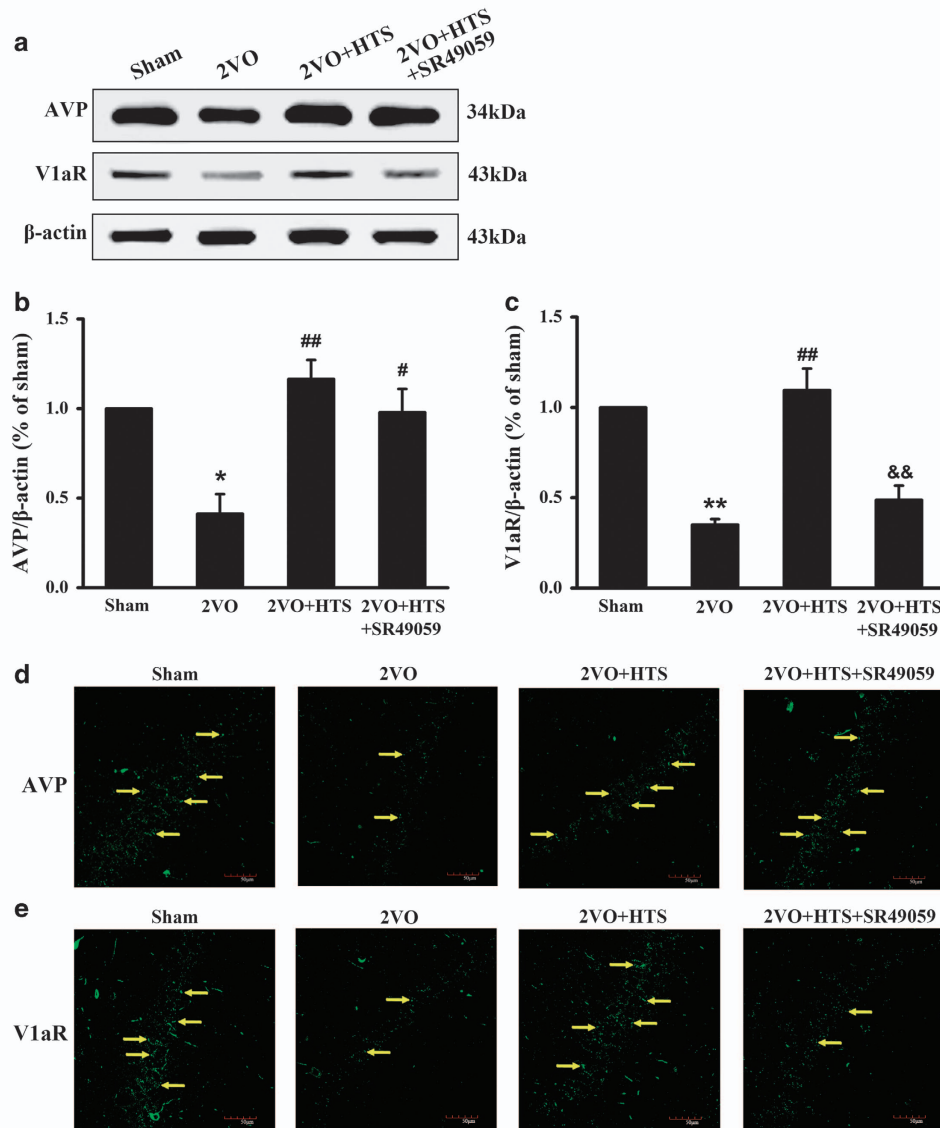


**Figure 1.** The expressions of AVP and V1aR in hippocampus of sham, 2VO, 2VO + HTS and 2VO + HTS + SR49059 groups. (a) Representative immunoreactive bands of AVP (34 kDa), V1aR (43 kDa) and  $\beta$ -actin (43 kDa). Proteins lysed in RIPA were loaded at 30  $\mu$ g per well. (b) Quantitative analysis of the optical density ratio of AVP/ $\beta$ -actin. (c) Quantitative analysis of the optical density ratio of V1aR/ $\beta$ -actin. Data are shown as mean  $\pm$  s.e.m. \* $P$  < 0.05, \*\* $P$  < 0.01 versus sham group; # $P$  < 0.05, ## $P$  < 0.01 versus 2VO group; && $P$  < 0.01 versus 2VO + HTS group (one-way ANOVA analysis followed by LSD test).  $n$  = 4 per group. (d) Representative immunofluorescence photographs of AVP in the hippocampal CA1 region. Yellow arrows denote V1a receptor expression. Scale bar = 50  $\mu$ m. ANOVA, analysis of variance; AVP, arginine vasopressin; HTS, hypertonic saline; LSD, least significant difference; 2VO, two vessel occlusion; V1aR, V1a receptor.

fluorescence by Alexa 488-conjugated anti-rabbit IgG. It was found that fluorescence intensity and larger numbers of bright fluorescent particles (yellow arrows) were visibly enhanced in the 2VO + HTS group, and SR49059 weakened fluorescence intensity of V1aR, which were consistent with the results of western blot assay in Figures 1a–c.

Endogenous AVP ameliorated spatial cognition partly through the V1aR signaling pathway

In order to detect the effect of endogenous AVP on spatial cognition, we used MWM test. As shown in Figures 2a and b, the mean escape latencies were decreased progressively in all four groups during the five training days without affecting swimming

speeds, which indicated the efficient learning processes. Moreover, 2VO rats spent significantly longer time to find the platform than rats in the sham group through the initial training stage (Figure 2a,  $P$  < 0.01 for day 1, day 3, day 4 and day 5;  $P$  < 0.05 for day 2). When considered the 2VO + HTS group, the escape latencies were rescued in a significant level from day 3 to day 5 (Figure 2a,  $P$  < 0.01 for day 3 and day 4;  $P$  < 0.05 for day 5). Interestingly, the escape latencies were remarkably prolonged from day 1 to day 5 under SR49059 compared with those of the 2VO + HTS group (Figure 2a,  $P$  < 0.05 for day 1, day 4 and day 5;  $P$  < 0.01 for day 2;  $P$  < 0.001 for day 3).

Furthermore, the swim traces of all four groups in the space exploring test were shown in Figure 2c. It can be seen

that both the platform crossings and the target quadrant dwell time were obviously decreased in the 2VO group compared with those in the sham group (Figures 2c–e,  $P < 0.01$  for the platform crossings;  $P < 0.001$  for the quadrant dwell time), but were significantly increased with the injection of HTS

(Figures 2c–e,  $P < 0.01$ ). However, they were reduced again in the 2VO + HTS + SR49059 group (Figures 2c–e,  $P < 0.01$ ). These results suggested that endogenous AVP improved the spatial learning and memory abilities in 2VO rats involved with V1aR.

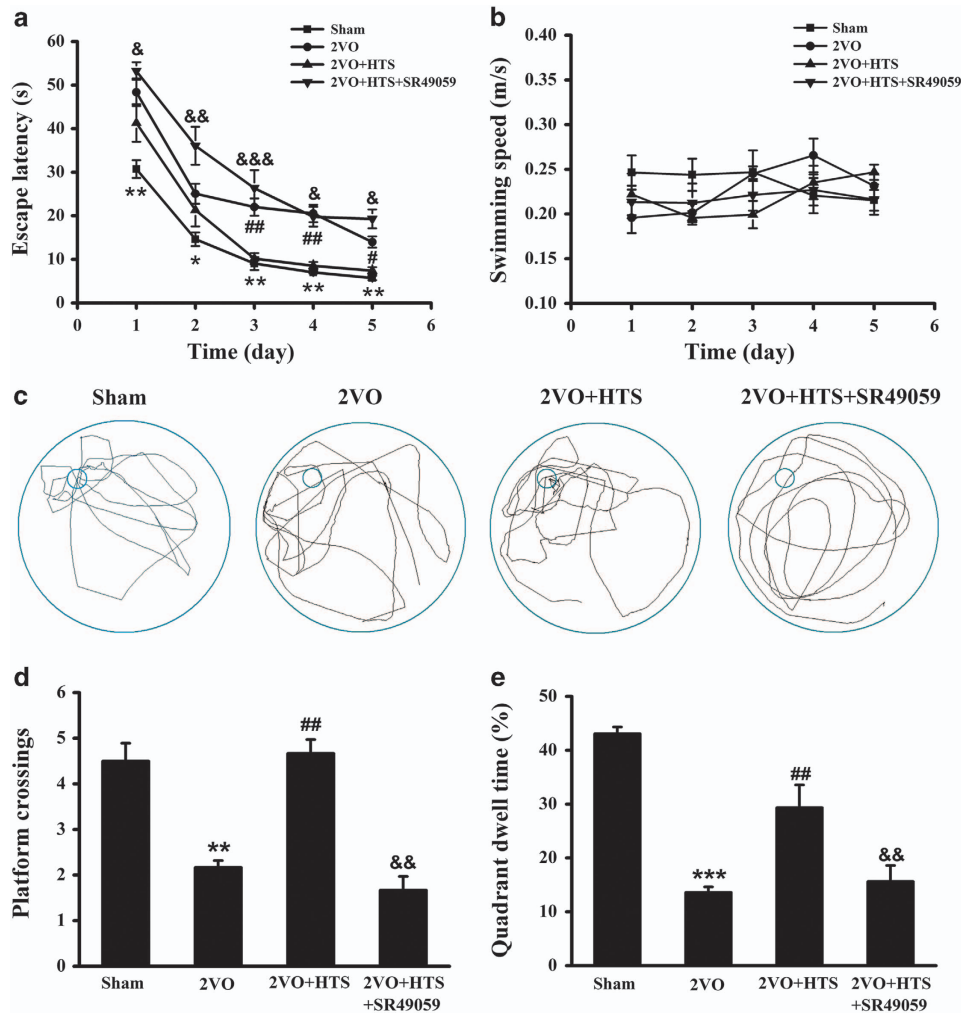


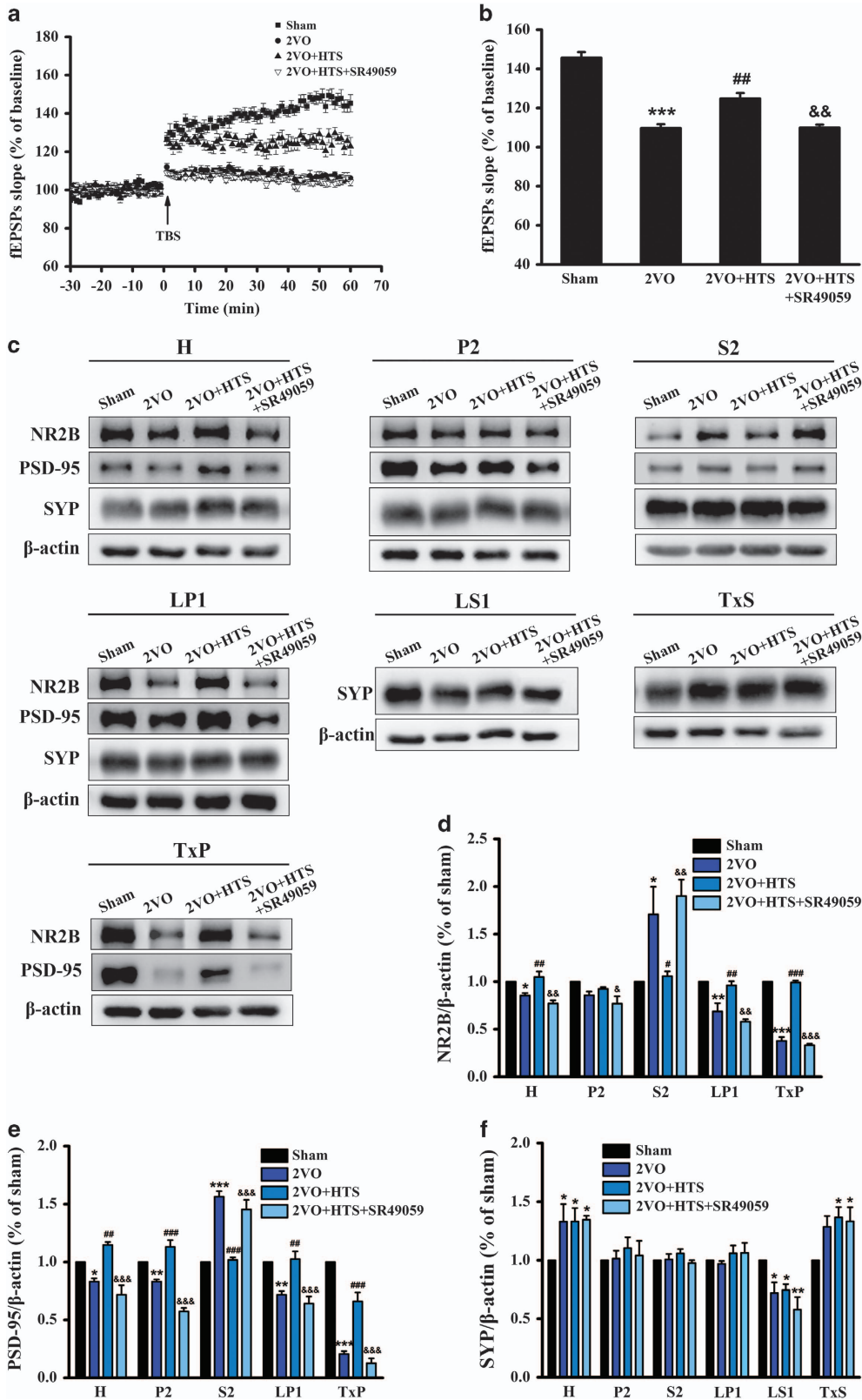
**Figure 2.** The performance of rats in IT and SET stages of MWM experiment. (a) Calculated escape latency on each day in IT stage of sham, 2VO, 2VO + HTS and 2VO + HTS + SR49059 groups (two-way repeated measures ANOVA with LSD or Dunnett's T3 *post hoc* test). (b) Swimming speeds on each day in the IT stage of four groups (two-way repeated measures ANOVA). (c) Representative swim traces of all four groups in SET stage. (d) The number of platform crossings in the SET stage (Mann–Whitney *U*-test). (e) Percentage of time spent in target quadrant (quadrant III) in SET stage (one-way ANOVA analysis followed by LSD test). Data are shown as mean  $\pm$  s.e.m. \* $P < 0.05$ , \*\* $P < 0.01$ , \*\*\* $P < 0.001$  versus sham group; # $P < 0.05$ , ## $P < 0.01$  versus 2VO group; & $P < 0.05$ , && $P < 0.01$ , &&& $P < 0.001$  versus 2VO + HTS group.  $n = 8$  per group. ANOVA, analysis of variance; HTS, hypertonic saline; IT, initial training; LSD, least significant difference; MWM, Morris water maze; SET, space exploring test; 2VO, two vessel occlusion.

**Figure 3.** Long-term potentiation (LTP) from Schaffer collaterals to the hippocampal CA1 and synaptic protein expressions in hippocampus of sham, 2VO, 2VO + HTS and 2VO + HTS + SR49059 groups. (a) The changes of time coursing in normalized fEPSP slopes in sham, 2VO, 2VO + HTS and 2VO + HTS + SR49059 groups. The first 30 min of evoked responses were normalised and used as the baseline responses of LTP. Arrow represents application of a theta burst stimulation (TBS). (b) The mean normalized fEPSP slopes between 45 and 60 min after the TBS.  $n = 8$  per group. (c) Representative immunoreactive bands of NR2B (180 kDa), PSD-95 (95 kDa), SYP (38 kDa) and  $\beta$ -actin (43 kDa) in different subcellular fractions. Proteins were loaded at 5  $\mu$ g per well for the LS1, 10  $\mu$ g per well for the H, P2, LP1, TxS and TxP and 30  $\mu$ g per well for the S2. (d–f) Quantitative analysis of the optical density ratio of NR2B/ $\beta$ -actin (d), PSD-95/ $\beta$ -actin (e) and SYP/ $\beta$ -actin (f) in different subcellular fractions. Data are shown as mean  $\pm$  s.e.m. \* $P < 0.05$ , \*\* $P < 0.01$ , \*\*\* $P < 0.001$  versus sham group; # $P < 0.05$ , ## $P < 0.01$ , ### $P < 0.001$  versus 2VO group; & $P < 0.05$ , && $P < 0.01$ , &&& $P < 0.001$  versus 2VO + HTS group (one-way ANOVA analysis followed by LSD test).  $n = 4$  per group. ANOVA, analysis of variance; fEPSP, field excitatory postsynaptic potential; HTS, hypertonic saline; LSD, least significant difference; NR2B, N-methyl-D-aspartate receptor subunit 2B; PSD-95, postsynaptic density protein 95; 2VO, two vessel occlusion.

Endogenous AVP improved synaptic plasticity and modulated synaptic protein expressions in the hippocampus relying on V1aR signaling pathway

To investigate the electrophysiological basis of MWM, LTP recording was performed, which indicated synaptic plasticity.

The time course of field excitatory postsynaptic potential (fEPSP) slopes that were normalized to the 30-min baseline period was presented in Figure 3a. The fEPSP slopes of four groups were increased immediately after theta burst stimulation and stabilized to different levels above the baseline period. Statistical mean



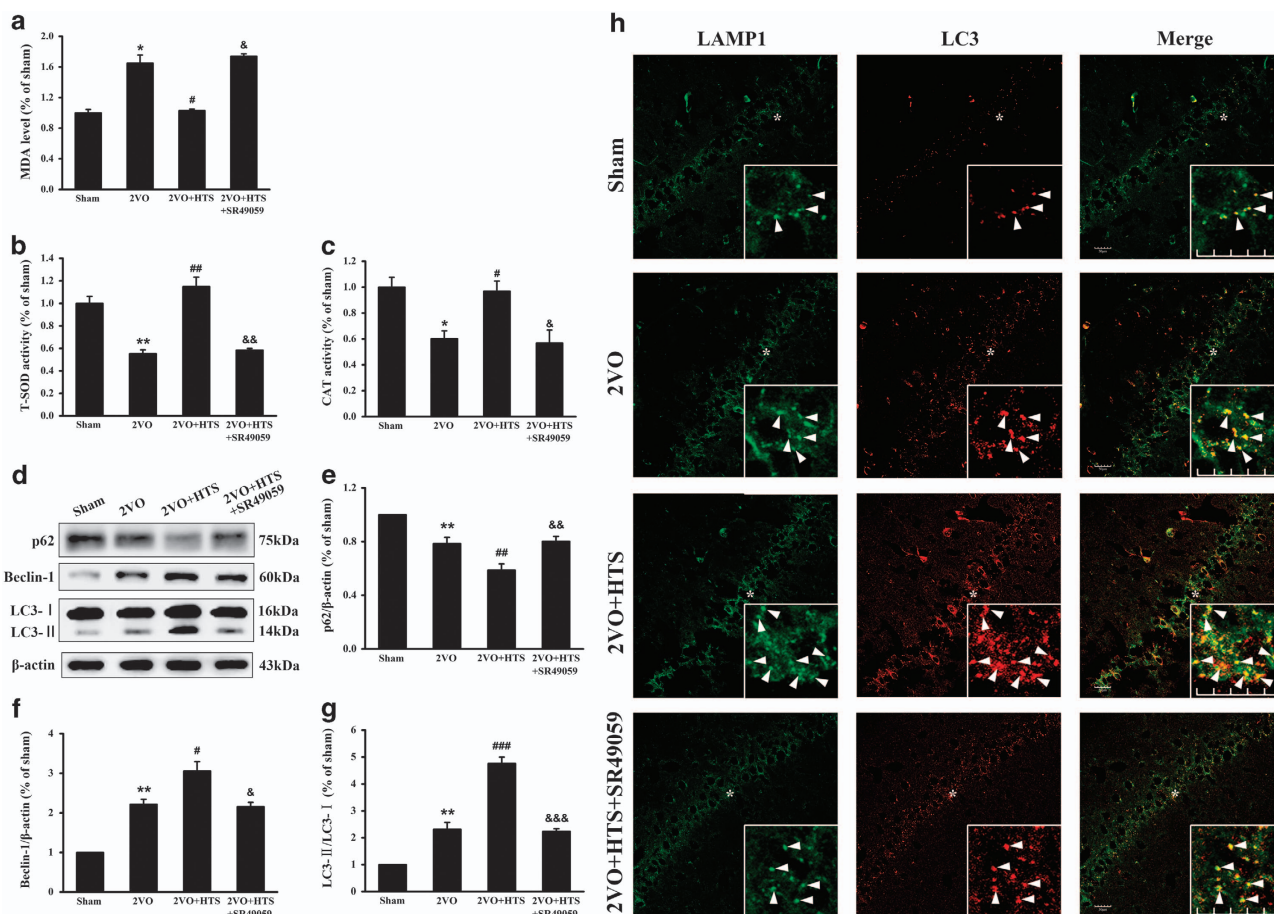


**Figure 4.** The changes of oxidative parameters and autophagy levels in the hippocampus of sham, 2VO, 2VO + HTS and 2VO + HTS + SR49059 groups. **(a)** The MDA level in hippocampus of the four groups (Mann–Whitney *U*-test). **(b)** The T-SOD activity in hippocampus of the four groups (one-way ANOVA analysis followed by LSD test). **(c)** The CAT activity in hippocampus of the four groups (one-way ANOVA analysis followed by LSD test). **(d)** Representative immunoreactive bands of SQSTM1/p62 (75 kDa), Beclin-1 (60 kDa), LC3-I (16 kDa), LC3-II (14 kDa) and β-actin (43 kDa). Proteins lysed in RIPA were loaded at 30 μg per well. **(e–g)** Quantitative analysis of the optical density ratio of p62/β-actin **(e)**, Beclin-1/β-actin **(f)**, and LC3-II/LC3-I **(g)**; one-way ANOVA analysis followed by LSD test). Data are shown as mean ± s.e.m. \**P* < 0.05, \*\**P* < 0.01 versus sham group; #*P* < 0.05, ##*P* < 0.01, ###*P* < 0.001 versus 2VO group; &*p* < 0.05, &&*p* < 0.01, &&&*p* < 0.001 versus 2VO + HTS group. *n* = 4 per group. **(h)** Representative immunofluorescence photographs showed the co-localization of LC3 and LAMP1 in CA1 regions as indicated by yellow punctiform staining. Higher magnification views of the areas marked with \* were shown as insets. White arrows denote LC3, LAMP1 and merged punctas. Scale bar = 50 μm. ANOVA, analysis of variance; CAT, catalase; HTS, hypertonic saline; LSD, least significant difference; MDA, malondialdehyde; T-SOD, total superoxide dismutase; 2VO, two vessel occlusion.

values of the last 15 min were shown in Figure 3b. The fEPSP slopes of 2VO rats were smaller than those of sham (*P* < 0.001) and HTS-treated rats (*P* < 0.01), and SR49059 was able to reduce the fEPSP slopes compared with those of HTS-treated rats (*P* < 0.01), which meant that endogenous AVP enhanced the impaired synaptic plasticity induced by 2VO partly through V1aR signaling pathway.

Synaptic protein levels are closely associated with cognitive function and synaptic plasticity, and are reported to be vulnerable to ischemia. In addition, NMDA receptors exhibit different properties owing to their different subcellular localization, whose trafficking has emerged as an important mechanism for modulation of synaptic function.<sup>43</sup> Thus, synaptic protein expressions in different subcellular domains were assessed by western blot assay. We carried out biochemical fractionation to isolate proteins from distinct subcellular compartments (Supplementary Figure S2A), and the effectiveness of the procedure was validated by confirming the unique expression patterns of protein markers of distinctive compartments (Supplementary Figure S2B). NR2B and PSD-95 were found enriched in the crude synaptosomal

membranes (P2), in the synaptosomal membranes (LP1) and in the Triton X-100-insoluble fraction (TxP), which contains the PSD. These proteins were also found in total homogenate (H), in the cytosol and microsomal membranes (S2), and in the synaptic vesicles (LS1) at low levels. However, NR2B as well as PSD-95 were undetectable in the Triton X-100-soluble fraction (TxS). The synaptic vesicle membrane protein synaptophysin, enriched in the presynaptic terminals, had a wider subcellular distribution except in the TxP.

As shown in Figures 3c–e, bilateral carotid arteries' occlusion reduced NR2B and PSD-95 levels in the H (*P* < 0.05), P2 (*P* = 0.054 for NR2B and *P* < 0.01 for PSD-95), LP1 (*P* < 0.01) and especially in the TxP (*P* < 0.001) fractions. However, 2VO increased NR2B and PSD-95 notably in the S2 (*P* < 0.05 for NR2B and *P* < 0.001 for PSD-95). Meanwhile, in 2VO rats, compared with sham, SYP was increased in the H (*P* < 0.05) and TxS (*P* = 0.051), but decreased in the LS1 (*P* < 0.05), and did not alter in the P2, S2 and LP1 (Figures 3c and f). After being administered with HTS, NR2B and PSD-95 levels were increased in the H (*P* < 0.01), P2 (*P* = 0.321 for NR2B and *P* < 0.001 for PSD-95), LP1 (*P* < 0.01) and TxP (*P* < 0.001)

fractions, and decreased in the S2 fraction ( $P < 0.05$  for NR2B and  $P < 0.001$  for PSD-95), as compared with those in 2VO rats (Figures 3c–e). Interestingly, these effects of HTS were abrogated upon SR49059 treatment (Figures 3c–e). No difference was found in the expression levels of SYP in any fraction between the 2VO, 2VO + HTS and 2VO + HTS + SR49059 groups (Figures 3c and f). These results disclosed altered NR2B, PSD-95 and SYP distributions in the synaptic compartments of the hippocampus in 2VO rats, and endogenous AVP affected postsynaptic proteins at a corresponding synaptic target relying on V1aR. The alteration of synaptic proteins might contribute to the changes in synaptic plasticity.

Endogenous AVP altered the level of Nissl bodies but not the morphology of pyramidal neurons

The Nissl body, which consists of a large number of rough endoplasmic reticulum and free ribosomes, is mainly to synthesize structural proteins and enzymes, so that detection of Nissl bodies is generally used as a key indicator of neuronal viability.<sup>44</sup> The expression of Nissl bodies was presented by either green point shape distribution or a green ring around the nucleus (yellow arrows) in Supplementary Figure S3A. Compared with the sham group, the Nissl bodies were reduced in the 2VO group, suggesting dysfunction of protein synthesis to some extent. However, the reduction was attenuated after HTS treatment. What's more, SR49059 canceled the effect of HTS.

Hematoxylin-eosin staining of the CA1 region was shown in Supplementary Figure S3B. Pyramidal cells were full, arranged tightly and the nuclei were light-stained in the sham group. However, in 2VO rats, the pyramidal cell layer was loosely arranged, the cell outline disappeared in many pyramidal cells and nuclear pyknosis was evident (Supplementary Figure S3B). There was no distinct difference between 2VO, 2VO + HTS and 2VO + HTS + SR49059 groups, indicating no improvement in the morphology of pyramidal neurons of HTS-treated rats.

Endogenous AVP reduced oxidative stress and upregulated autophagy partially through activation of V1aR signaling in a 2VO rat model

It is generally known that oxidative stress is one of the main damage that occurs after 2VO procedure. Therefore, we measured the effects of endogenous AVP on the MDA level, total superoxide dismutase and catalase activities in the hippocampus. The results presented that the MDA level was significantly elevated in the 2VO group compared with that in the sham group (Figure 4a,  $P < 0.05$ ), whereas HTS could downregulate the elevated MDA level (Figure 4a,  $P < 0.05$ ), and, when treated with SR49059, the MDA level reverted to the level in the 2VO group (Figure 4a,  $P < 0.05$ ). Moreover, the total superoxide dismutase and catalase activities changed in an opposite way against the MDA level (Figures 4b and c). Our results revealed the antioxidant effect of endogenous AVP in 2VO rats partly through the V1aR signaling pathway.

A previous study reported that autophagy was closely related to oxidative stress, which led us to assess the effects of AVP on the expressions of autophagy-related markers Beclin-1, LC3 and SQSTM1/p62. It can be seen that the expression of Beclin-1 was increased observably in the 2VO group (Figures 4d and f,  $P < 0.01$  versus sham). After being treated with HTS, there was a further increase of Beclin-1 expression compared to that of 2VO group (Figures 4d and f,  $P < 0.05$ ). However, the elevation in the expression of Beclin-1 was decreased upon SR49059 treatment (Figures 4d and f,  $P < 0.05$ ). The similar results were obtained in the measurement of LC3-II/LC3-I levels (Figures 4d and g). These data revealed increasing autophagosome levels induced by 2VO and HTS, which involved with V1aR for the latter. Furthermore, the autophagic substrate, SQSTM1/p62, was reduced by 2VO (Figures 4d and e,  $P < 0.01$ ), and was further decreased by HTS

(Figures 4d and e,  $P < 0.01$  versus 2VO), which corresponded to an activation of the autophagic flux induced by 2VO and HTS. Likewise, the increase in the p62 protein level in the 2VO + HTS + SR49059 group (Figures 4d and e,  $P < 0.01$  versus 2VO + HTS) demonstrated HTS-promoting autophagic flux through V1aR.

We then performed double immunofluorescence to detect the co-stains for LC3 and lysosomal marker LAMP1 in CA1 regions, which indicated the fusion of autophagosomes with lysosomes. As shown in Figure 4h, the red punctas of LC3 (LC3-II) were more abundant in 2VO compared with those in sham, and were further upregulated by HTS. Besides, in the 2VO + HTS group, these red punctas were highly enriched within LAMP1-positive structures (green) as indicated by yellow punctiform staining, thus describing the fusion between autophagosomes and lysosomes to generate autolysosomes. However, the red punctas of LC3 were decreased in the 2VO + HTS + SR49059 group compared with those in 2VO + HTS group; as a result, the co-localization between LC3 and LAMP1 was reduced. Collectively, the results of this experiment as well as expressions of Beclin-1, LC3 and SQSTM1/p62 were basically sufficient to determine a real enhancement of the autophagy flux induced by 2VO and HTS, and V1aR was crucial to the effect of HTS.

## DISCUSSION

CCH is able to bring about diminished production of certain hormones and neurotransmitters. Previous studies have shown, in most of the vascular dementia cases characterized by CCH, the reduction of the AVP mRNA level in the supraoptic nucleus (SON), besides the reduction of AVP in the hippocampus, which were related to cognitive decline.<sup>45,46</sup> The possible reason behind the decrease in AVP levels in SON was abundant peripheral lipofuscin accumulations in SON neurons, which influenced the function of AVP neurons. Moreover, vasopressin fibers of the magnocellular hypothalamic nuclei project to the hippocampus,<sup>47</sup> making the AVP-containing neurons of the magnocellular nuclei an important source for hippocampal AVP innervation;<sup>48</sup> this could explain why AVP reduction occurred in the hippocampus. These findings were consistent with ours, and could explain them to some extent. The study previously reported the most important stimulus for AVP secretion to be hyperosmolality.<sup>33</sup> Therefore, in our study, the hypertonic saline was intended to upregulate the hippocampal AVP through activating the hypothalamic, osmotic-sensitive magnocellular AVP system,<sup>49</sup> but not to induce its release to peripheral regions by allowing the rats to drink *ad libitum* during the last 10 min before MWM or LTP recording.<sup>48</sup> In addition, another mechanism about hypertonic saline inducing AVP reported by Yoshida<sup>50</sup> was that the osmotic stimuli mediated the rapid transcriptional induction of the vasopressin gene via increasing Fos protein mRNAs. These findings also verified our results in Figures 1a, b and d that intraperitoneal administration of 5.3% (900 mOsm) saline (2% of body weight) was able to induce an endogenous AVP increase in the hippocampus.

MWM test has been a standard experiment to study the spatial learning and memory. Our results from the MWM test inferred that spatial learning and reference memory were significantly impaired in 2VO rats, which were in line with the results of Li *et al.*<sup>39</sup> and Zhang *et al.*<sup>51</sup> We also discovered that endogenous AVP effectively alleviated cognitive deficiency induced by 2VO through V1aR signaling partially. Unexpectedly, however, Everts *et al.*<sup>52</sup> once delivered AVP antagonist d(CH2)5-D-Tyr(Et)VAVP (which was used to block all AVP receptors) bilaterally into the lateral septum in male Wistar rats, and found that there was no effect on spatial learning (MWM). Besides, Koshimizu *et al.*<sup>53</sup> reviewed that both V1aR-KO and V1bR-KO mice performed normally in a MWM. It is possible that these discrepancies between their results and ours are due to the different brain regions that focused on, slightly different strain backgrounds of experimental animals and different

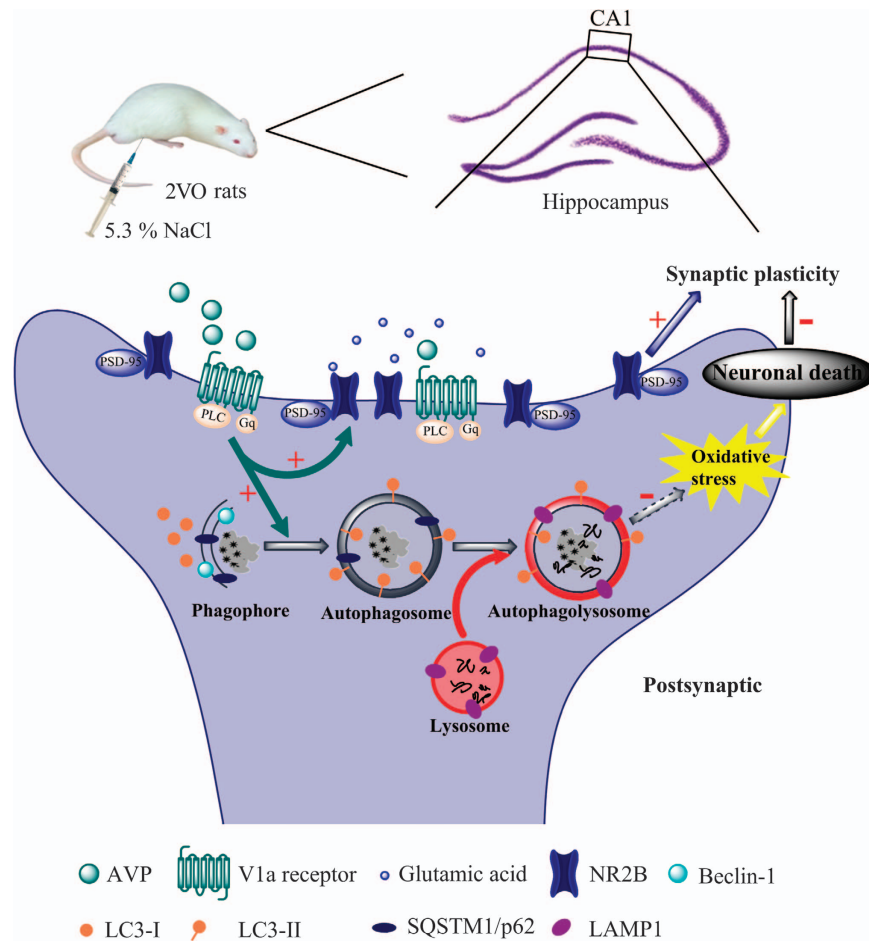


**Figure 5.** The underlying mechanisms that AVP ameliorates spatial learning impairments. The red '+' represented the enhancement effect; the red '-' represented the inhibiting effect; the dashed arrow represented the process, which was not verified in our study. AVP, arginine vasopressin.

testing procedures. Moreover, the 2VO rat model we used, which is different from their studies, may contribute to these discrepancies especially. Therefore, it is clear in our present study that the V1aR in hippocampus is important for AVP, alleviating impairments of spatial learning and memory in 2VO rats.

LTP from Schaffer collaterals to the hippocampal CA1 region was carried out considering the distribution of V1aR in the present study. Our data implied that the synaptic plasticity was significantly impaired in 2VO rats, which was in accordance with the findings of previous studies.<sup>39,54,55</sup> Interestingly, the negative effect of 2VO on LTP was notably attenuated after treating with hypertonic saline (Figures 3a and b). Study by Rong *et al.*<sup>11</sup> illustrated that AVP4-8 could induce a long-lasting potentiation effect on the evoked EPSP and enhance LTP in the CA1 and CA3 fields of the dorsal hippocampus due to a presynaptic mechanism of action, which partially supported our findings *in vitro*. Furthermore, our data that SR49059 abolished the effect of AVP (Figures 3a and b) indicated that endogenous AVP improved the synaptic plasticity relying on V1aR in the hippocampus. The result of LTP was paralleled with MWM performance, which was supported by the notion that changes in synaptic efficacy underlie learning and memory processes.<sup>56</sup>

Clayton *et al.* reported that knocking down NR2B expression abolished LTP and impaired spatial learning, demonstrating the important role of NR2B in LTP and learning and memory.<sup>57</sup> Almost all NR2B subunits are reportedly found in the plasma membrane

so that they participate in neurotransmission. At the postsynaptic membrane of excitatory synapses, NMDARs are attached to the PSD that delicately regulate synaptic plasticity, which is known as LTP or LTD (long-term depression).<sup>58</sup> In our study, we found that NR2B expression was reduced in total homogenate (H) and especially in the PSD (TxP) after CCH (Figures 3c and d), which may have distinctly direct effects on synaptic plasticity. It was likely that an overall inhibition of new NR2B protein synthesis could account for the NR2B reduction. Our results in which the Nissl bodies were reduced in 2VO (Supplementary Figure S3A), and in a previous study that reported hippocampal NR2B mRNA and protein expression in 2VO were decreased,<sup>59</sup> could confirm our viewpoint. In contrast, NR2B in the intracellular pools (S2) containing endoplasmic reticulum/Golgi apparatus involved in synthesis, assembly and secretion of proteins was upregulated in 2VO rats (Figures 3c and d). The number of NMDARs stabilized at the cell surface represents a balance between internalization and insertion. As the surface:intracellular ratio of NR2B was reduced, the fact that the NR2B upregulation in the S2 implied a scenario, in which trafficking or delivery of NR2B from the S2 to the TxP was suppressed or the removal of NR2B from the TxP was accelerated.<sup>60</sup> The reduced surface:intracellular ratio of NR2B may also contribute to the impaired LTP, as, to our knowledge, Grosshans *et al.*<sup>61</sup> first demonstrated that the rapid insertion of new NMDARs from intracellular pools to the postsynaptic membrane underlies LTP. It has been well established that



PSD-95, which anchors and clusters postsynaptic glutamate receptors,<sup>62,63</sup> stabilizes surface NR2B and inhibits NR2B internalization.<sup>64,65</sup> The expression of PSD-95 changed in the same way as NR2B (Figures 3c and e); thus impairing PSD-95 in the TxP may support the scenario regarding accelerated NR2B internalization.

Administration of hypertonic saline, which increased endogenous AVP in the hippocampus, was capable of upregulating the surface:intracellular ratio of NR2B relying on V1aR (Figures 3c and d). These data illustrated that AVP promoted NR2B trafficking to the plasma membrane, or slowed down the internalization of NR2B. The elevated PSD-95 level might also enhance the surface expression of NR2B. The redistribution of NR2B and PSD-95 caused by AVP contributed to the enhanced LTP. A previous study reported that the activation of PKC enhanced NMDA channel opening and rapid insertion at the surface of hippocampal neurons.<sup>66</sup> Besides, a major signaling pathway triggered by V1aRs is activation of phospholipase C and PKC.<sup>67</sup> Thus, although the role of PKC was not examined in the present study, it was likely that AVP altered the distribution of NR2B and PSD-95 through the V1aR/phospholipase C/PKC signaling pathway.

With respect to SYP, which was closely related to the release of neurotransmitters,<sup>68</sup> there were increases in the H and TxS in 2VO rats (Figures 3c and f). These results differed from Wang *et al.*,<sup>69</sup> which showed decreased SYP in 2VO. As the induction of 2VO was the same, the apparent discrepancy can be related to the different strain backgrounds and different ages of rats, as well as different protein extraction methods used. Unlike NR2B and PSD-95, SYP was barely affected by hypertonic saline with or without SR49059 (Figures 3c and f). In consequence, we concluded that endogenous AVP enhanced the LTP mainly by postsynaptic mechanisms through V1aR signaling.

In general, the autophagic pathway operates at low levels under normal conditions, but is rapidly upregulated under stress conditions, such as oxidative stress, starvation and hormonal imbalances. In the current study, our results showed that autophagy was activated under 2VO-induced ischemic stress (Figures 4d–h), which were in accordance with previous studies.<sup>70–72</sup> Surprisingly, we found that endogenous AVP further elevated the level of autophagy based on 2VO, and then SR49059 brought it back to the level similar to the 2VO group (Figures 4d–h), which indicated that endogenous AVP enhanced autophagy via V1aR signaling in the 2VO model rat. The possible mechanism was that AVP activated AMP-activated protein kinase via Ca<sup>2+</sup> signaling, thus triggering autophagy through directly activating UNC-51-like kinase 1 (ULK1) and indirectly inhibiting the suppressive effect of mammalian target of rapamycin complex 1 on ULK1. This signaling pathway has been confirmed in previous studies in H9c2 cells.<sup>73,74</sup> Certainly, an additional investigation of this signal pathway *in vitro* will strengthen our understanding of the relationships between AVP and autophagy.

In recent years, there has been a growing interest in the role of autophagy in cerebral ischemia. It is believed that autophagy in CNS is a double-edged sword, as the contribution of autophagy to neuronal death/survival is still controversial. In our study, AVP attenuated oxidative stress (Figures 4a–c) and increased Nissl bodies (Supplementary Figure S3A). Besides, researches demonstrated that macroautophagy and chaperone-mediated autophagy were activated in response to oxidative stress, removing the damaged components before further damage or aggregation occurs.<sup>75–77</sup> Thus, we tentatively proposed that the autophagy enhanced by AVP acted as a defender to protect neuronal cells against 2VO-induced oxidative stress and consequential neuronal death. To confirm our interpretation, further investigation using autophagy inducers and inhibitors should be carried out systematically. Our viewpoint was consistent with some studies, which claimed that autophagy activation is associated with neuroprotection in cerebral ischemia.<sup>22–24</sup> However, in contrast to these and

our results, Koike *et al.*<sup>26</sup> found that autophagy induced hypoxic-ischemic injury-mediated neuronal death execution, using mice deficient in Atg7. Their viewpoint was supported by several other independent groups.<sup>27–29</sup> Differences in the animal strain utilized, the experimental approach, the brain area analyzed and especially the modeling method and the timing of analysis may account for this discrepancy. Anyway, the mechanism of how neurons regulate the two opposite downstream effects of autophagy, survival and death after CCH deserves further investigation.

In summary, our study reported that endogenous AVP induced by osmotic stimulus was effective in alleviating spatial learning and memory deficits at least partly through V1aR signaling in 2VO rats (Figure 2). The underlying mechanisms, as shown in Figure 5, were that AVP promoted NR2B and PSD-95 externalization, and enhanced autophagy via V1aR (Figures 4d–h), which might uncover a brand new protective mechanism of AVP that possibly involved in reducing oxidative stress (Figures 4a–c) and sequentially enhancing neuronal viability (Supplementary Figure S3A). The above two aspects could contribute to attenuating the impairment of synaptic plasticity (Figures 3a and b), which was closely related to spatial learning and memory. Although there are important discoveries in our study, there are limitations also. Further investigation is needed to explore whether autophagy plays a definite protective role in the 2VO model by regulating the autophagy level. Our data revealed the mechanisms of the neuroprotection of AVP against 2VO-induced cognitive impairments, which might be used as a therapeutic method for conditions involving CCH, such as mild cognitive impairment, vascular dementia and Alzheimer's disease. The results of this study also imply that autophagy may serve as a potential novel target for pharmacological intervention in CCH.

## CONFLICT OF INTEREST

The authors declare no conflict of interest.

## ACKNOWLEDGMENTS

This work was supported by the Applied Basic Research Programs of Science and Technology Commission Foundation of Tianjin (14JCZDJC35000) and Grant from the National Natural Science Foundation of China (81571804).

## REFERENCES

- Farkas E, Luiten PG, Bari F. Permanent, bilateral common carotid artery occlusion in the rat: a model for chronic cerebral hypoperfusion-related neurodegenerative diseases. *Brain Res Rev* 2007; **54**: 162–180.
- Román GC. Brain hypoperfusion: a critical factor in vascular dementia. *Neurol Res* 2004; **26**: 454–458.
- Fotuhi M, Hachinski V, Whitehouse PJ. Changing perspectives regarding late-life dementia. *Nat Rev Neurol* 2009; **5**: 649–658.
- De la Torre J, Fortin T. A chronic physiological rat model of dementia. *Behav Brain Res* 1994; **63**: 35–40.
- Torre JC, Fortin T, Park GAS, Pappas BA, Richard MT. Brain blood flow restoration 'rescues' chronically damaged rat CA1 neurons. *Brain Res* 1993; **623**: 6–15.
- Raggenbass M. Overview of cellular electrophysiological actions of vasopressin. *Eur J Pharmacol* 2008; **583**: 243–254.
- Bielsky IF, Hu SB, Ren X, Terwilliger EF, Young LJ. The V1a vasopressin receptor is necessary and sufficient for normal social recognition: a gene replacement study. *Neuron* 2005; **47**: 503–513.
- Raggenbass M. Vasopressin- and oxytocin-induced activity in the central nervous system: electrophysiological studies using in-vitro systems. *Progr Neurobiol* 2001; **64**: 307–326.
- Young WS, Li J, Wersinger SR, Palkovits M. The vasopressin 1b receptor is prominent in the hippocampal area CA2 where it is unaffected by restraint stress or adrenalectomy. *Neuroscience* 2006; **143**: 1031–1039.
- Chepkova AN, French P, Wied DD, Ontskul AH, Ramakers GMJ, Skrebitski VG *et al*. Long-lasting enhancement of synaptic excitability of CA1/subiculum neurons of the rat ventral hippocampus by vasopressin and vasopressin(4–8). *Brain Res* 1995; **701**: 255–266.

- 11 Rong XW, Chen XF, Du YC. Potentiation of synaptic transmission by neuropeptide AVP4-8 (ZNC(C)PR) in rat hippocampal slices. *Neuroreport* 1993; **4**: 1135–1138.
- 12 Dubrovsky B, Tatarinov AK, Harris J, Tsiodras A. Effects of arginine-vasopressin (AVP) on long-term potentiation in intact anesthetized rats. *Brain Res Bull* 2003; **59**: 467–472.
- 13 Egashira N, Tanoue A, Higashihara F, Mishima K, Fukue Y, Takano Y et al. V1a receptor knockout mice exhibit impairment of spatial memory in an eight-arm radial maze. *Neurosci Lett* 2004; **356**: 195–198.
- 14 Klionsky DJ, Emr SD. Autophagy as a regulated pathway of cellular degradation. *Science* 2000; **290**: 1717–1721.
- 15 Wagner C. Loss of autophagy in the central nervous system causes neurodegeneration in mice. *Nature* 2006; **441**: 880–884.
- 16 Mccray BA, Taylor JP. The role of autophagy in age-related neurodegeneration. *Neurosignals* 2008; **16**: 75–84.
- 17 Liu L, Li C-J, Lu Y, Zong X-G, Luo C, Sun J et al. Baclofen mediates neuroprotection on hippocampal CA1 pyramidal cells through the regulation of autophagy under chronic cerebral hypoperfusion. *Sci Rep* 2015; **5**: 14474.
- 18 Qin ZH, Wang Y, Kegel KB, Kazantsev A, Apostol BL, Thompson LM et al. Autophagy regulates the processing of amino terminal huntingtin fragments. *Hum Mol Genet* 2003; **12**: 3231–3244.
- 19 Ana Maria C, Leonidas S, Ross F, Lansbury PT, David S. Impaired degradation of mutant  $\alpha$ -synuclein by chaperone-mediated autophagy. *Science* 2004; **305**: 1292–1295.
- 20 Taichi H, Kenji N, Makoto M, Akitsugu Y, Yohko N, Rika SM et al. Suppression of basal autophagy in neural cells causes neurodegenerative disease in mice. *Nature* 2006; **441**: 885–889.
- 21 Rubinsztein DC, Difiglia M, Heintz N, Nixon RA, Qin ZH, Ravikumar B et al. Autophagy and its possible roles in nervous system diseases, damage and repair. *Autophagy* 2005; **1**: 11–22.
- 22 Carloni S, Buonocore G, Balduini W. Protective role of autophagy in neonatal hypoxia-ischemia induced brain injury. *Neurobiol Dis* 2008; **32**: 329–339.
- 23 Wang P, Guan Y-F, Du H, Zhai Q-W, Su D-F, Miao C-Y. Induction of autophagy contributes to the neuroprotection of nicotinamide phosphoribosyltransferase in cerebral ischemia. *Autophagy* 2012; **8**: 77–87.
- 24 Sheng R, Zhang L-S, Han R, Liu X-Q, Gao B, Qin Z-H. Autophagy activation is associated with neuroprotection in a rat model of focal cerebral ischemic preconditioning. *Autophagy* 2010; **6**: 482–494.
- 25 Maiuri MC, Zalckvar E, Kimchi A, Kroemer G. Self-eating and self-killing: crosstalk between autophagy and apoptosis. *Nat Rev Mol Cell Biol* 2007; **8**: 741–752.
- 26 Koike M, Shibata M, Tadakoshi M, Gotoh K, Komatsu M, Waguri S et al. Inhibition of autophagy prevents hippocampal pyramidal neuron death after hypoxic-ischemic injury. *Am J Pathol* 2008; **172**: 454–469.
- 27 Ginet V, Spiehlmann A, Rummel C, Rudinskiy N, Grishchuk Y, Luthi-Carter R et al. Involvement of autophagy in hypoxic-excitotoxic neuronal death. *Autophagy* 2014; **10**: 846–860.
- 28 Liu Y, Shoji-Kawata S, Sumpster RM, Wei Y, Ginet V, Zhang L et al. Autosis is a Na<sup>+</sup>, K<sup>+</sup>-ATPase-regulated form of cell death triggered by autophagy-inducing peptides, starvation, and hypoxia-ischemia. *Proc Natl Acad Sci USA* 2013; **110**: 20364–20371.
- 29 Xie C, Ginet V, Sun Y, Koike M, Zhou K, Li T et al. Neuroprotection by selective neuronal deletion of Atg7 in neonatal brain injury. *Autophagy* 2016; **12**: 410–423.
- 30 Yang J, Yao Y, Chen T, Zhang T. VEGF ameliorates cognitive impairment in vivo and in vitro ischemia via improving neuronal viability and function. *Neuromol Med* 2014; **16**: 376–388.
- 31 Gal SL, Wagnon J, Garcia C, Lacour C, Guiraudou P, Christophe B, et al. Biochemical and pharmacological properties of SR 49059, a new, potent, nonpeptide antagonist of rat and human vasopressin V1a receptors. *J Clin Invest* 1993; **92**: 224–231.
- 32 Hernandez VS, Ruiz-Velazco S, Zhang L. Differential effects of osmotic and SSR149415 challenges in maternally separated and control rats: the role of vasopressin on spatial learning. *Neurosci Lett* 2012; **528**: 143–147.
- 33 Dunn FL, Brennan TJ, Nelson AE, Robertson GL. The role of blood osmolality and volume in regulating vasopressin secretion in the rat. *J Clin Invest* 1973; **52**: 3212–3219.
- 34 Landgraf R, Neumann I, Schwarzberg H. Central and peripheral release of vasopressin and oxytocin in the conscious rat after osmotic stimulation. *Brain Res* 1988; **457**: 219–225.
- 35 Manaenko A, Fathali N, Khatibi NH, Lekic T, Shum KJ, Martin R et al. Post-treatment with SR49059 improves outcomes following an intracerebral hemorrhagic stroke in mice. In: Zhang J, Colohan A (eds). *Intracerebral hemorrhage research. Acta Neurochirurgica Supplementum*. Springer: Vienna, Austria, 2011, pp 191–196.
- 36 Serradeil-Le Gal C, Wagnon J, Garcia C, Lacour C, Guiraudou P, Christophe B et al. Biochemical and pharmacological properties of SR 49059, a new, potent, non-peptide antagonist of rat and human vasopressin V1a receptors. *J Clin Invest* 1993; **92**: 224.
- 37 Yang J, An L, Yao Y, Yang Z, Zhang T. Melamine impairs spatial cognition and hippocampal synaptic plasticity by presynaptic inhibition of glutamatergic transmission in infant rats. *Toxicology* 2011; **289**: 167–174.
- 38 Quan M-N, Zhang N, Wang Y-Y, Zhang T, Yang Z. Possible antidepressant effects and mechanisms of memantine in behaviors and synaptic plasticity of a depression rat model. *Neuroscience* 2011; **182**: 88–97.
- 39 Li Z, Wang Y, Xie Y, Yang Z, Zhang T. Protective effects of exogenous hydrogen sulfide on neurons of hippocampus in a rat model of brain ischemia. *Neurochem Res* 2011; **36**: 1840–1849.
- 40 Gao J, Zhang X, Yu M, Ren G, Yang Z. Cognitive deficits induced by multi-walled carbon nanotubes via the autophagic pathway. *Toxicology* 2015; **337**: 21–29.
- 41 Hallett PJ, Collins TL, Standaert DG, Dunah AW. Biochemical fractionation of brain tissue for studies of receptor distribution and trafficking. *Curr Protoc Neurosci* 2008; **Chapter 1**, Unit 1.16.
- 42 Won S, Incontro S, Nicoll RA, Roche KW. PSD-95 stabilizes NMDA receptors by inducing the degradation of STEP61. *Proc Natl Acad Sci USA* 2016; **113**: E4736–E4744.
- 43 Grosshans DR, Clayton DA, Coultrap SJ, Browning MD. LTP leads to rapid surface expression of NMDA but not AMPA receptors in adult rat CA1. *Nat Neurosci* 2002; **5**: 27–33.
- 44 Li J, Wen PY, Li WW, Zhou J. Upregulation effects of Tanshinone IIA on the expressions of NeuN, Nissl body, and I $\kappa$ B and downregulation effects on the expressions of GFAP and NF- $\kappa$ B in the brain tissues of rat models of Alzheimer's disease. *Neuroreport* 2015; **26**: 758–66.
- 45 Ishunina TA, Wouter K, Swaab DF. Metabolic alterations in the hypothalamus and basal forebrain in vascular dementia. *J Neuropathol Exp Neurol* 2004; **63**: 1243–1254.
- 46 Li X, Zhou M, Li Y, Huang W, Li D, Duan J et al. Effect of Xingnaojing on somatostatin and arginine vasopressin in rats with vascular dementia. *African J Pharm Pharmacol* 2012; **6**: 474–479.
- 47 Buijs RM. Immunocytochemical demonstration of vasopressin and oxytocin in the rat brain by light and electron microscopy. *J Histochem Cytochem* 1980; **28**: 357–360.
- 48 Zhang L, Hernandez VS. Synaptic innervation to rat hippocampus by vasopressin-immuno-positive fibres from the hypothalamic supraoptic and paraventricular nuclei. *Neuroscience* 2013; **228**: 139–162.
- 49 Robertson GL, Shelton RL, Athar S. The osmoregulation of vasopressin. *Kidney Int* 1976; **10**: 25–37.
- 50 Yoshida M. Gene regulation system of vasopressin and corticotropin-releasing hormone. *Gene Regul Syst Biol* 2008; **2**: 71–88.
- 51 Zhang LM, Jiang CD. Hydrogen sulfide attenuates neuronal injury induced by vascular dementia via inhibiting apoptosis in rats. *Neurochem Res* 2009; **34**: 1984–1992.
- 52 Everts HG, Koolhaas JM. Differential modulation of lateral septal vasopressin receptor blockade in spatial learning, social recognition, and anxiety-related behaviors in rats. *Behav Brain Res* 1999; **99**: 7–16.
- 53 Koshimizu TA, Nakamura K, Egashira N, Hiroyama M, Nonoguchi H, Tanoue A. Vasopressin V1a and V1b receptors: from molecules to physiological systems. *Physiol Rev* 2012; **92**: 1813–1864.
- 54 Yao Y, Han DD, Zhang T, Yang Z. Quercetin improves cognitive deficits in rats with chronic cerebral ischemia and inhibits voltage-dependent sodium channels in hippocampal CA1 pyramidal neurons. *Phytother Res* 2010; **24**: 136–140.
- 55 Yang HY, Yang L, Xie JC, Liu NN, Xin T. Effects of repetitive transcranial magnetic stimulation on synaptic plasticity and apoptosis in vascular dementia rats. *Behav Brain Res* 2015; **281**: 149–155.
- 56 Martin S, Morris R. New life in an old idea: the synaptic plasticity and memory hypothesis revisited. *Hippocampus* 2002; **12**: 609–636.
- 57 Clayton DA, Mesches MH, Alvarez E, Bickford PC, Browning MD. A hippocampal NR2B deficit can mimic age-related changes in long-term potentiation and spatial learning in the Fischer 344 rat. *J Neurosci* 2002; **22**: 3628–3637.
- 58 Kennedy MB. Signal-processing machines at the postsynaptic density. *Science* 2000; **290**: 750–754.
- 59 Huang L, He Z, Guo L, Wang H. Improvement of cognitive deficit and neuronal damage in rats with chronic cerebral ischemia via relative long-term inhibition of rho-kinase. *Cell Mol Neurobiol* 2008; **28**: 757–768.
- 60 Mao L-M, Wang W, Chu X-P, Zhang G-C, Liu X-Y, Yang Y-J et al. Stability of surface NMDA receptors controls synaptic and behavioral adaptations to amphetamine. *Nat Neurosci* 2009; **12**: 602–610.
- 61 Grosshans D, Clayton D, Coultrap S, Browning M. LTP leads to rapid surface expression of NMDA but not AMPA receptors in adult rat CA1. *Nat Neurosci* 2002; **5**: 27–33.
- 62 Jean-Claude BQ, Rodrigo A. PSD-95 regulates synaptic transmission and plasticity in rat cerebral cortex. *J Physiol* 2003; **546**: 859–867.
- 63 Migaud M, Charlesworth P, Dempster M, Webster LC, Watabe AM, Makhinson M et al. Enhanced long-term potentiation and impaired learning in mice with mutant postsynaptic density-95 protein. *Nature* 1998; **396**: 433–439.

- 64 Roche KW, Standley S, McCallum J, Ly CD, Ehlers MD, Wenthold RJ. Molecular determinants of NMDA receptor internalization. *Nat Neurosci* 2001; **4**: 794.
- 65 Chung HJ, Huang YH, Lau L-F, Huganir RL. Regulation of the NMDA receptor complex and trafficking by activity-dependent phosphorylation of the NR2B subunit PDZ ligand. *J Neurosci* 2004; **24**: 10248–10259.
- 66 Lan J-y, Skeberdis VA, Jover T, Grooms SY, Lin Y, Araneda RC *et al*. Protein kinase C modulates NMDA receptor trafficking and gating. *Nat Neurosci* 2001; **4**: 382–390.
- 67 Birbaumer M. Vasopressin receptors. *Trends Endocrinol Metab* 2000; **11**: 406–410.
- 68 Aisa B, Elizalde N, Tordera R, Lasheras B, Río JD, Ramírez MJ. Effects of neonatal stress on markers of synaptic plasticity in the hippocampus: implications for spatial memory. *Hippocampus* 2009; **19**: 1222–1231.
- 69 Wang X, Xing A, Xu C, Cai Q, Liu H, Li L. Cerebrovascular hypoperfusion induces spatial memory impairment, synaptic changes, and amyloid- $\beta$  oligomerization in rats. *J Alzheimers Dis* 2010; **21**: 813–822.
- 70 Farré JC, Subramani S. Peroxisome turnover by micropexophagy: an autophagy-related process. *Trends Cell Biol* 2004; **14**: 515–523.
- 71 Guido K, Marja JT. Lysosomes and autophagy in cell death control. *Nat Rev Cancer* 2005; **5**: 886–897.
- 72 Kundu M, Thompson CB. Autophagy: basic principles and relevance to disease. *Annu Rev Pathol Mech Dis* 2008; **3**: 427–455.
- 73 Saeedi R, Saran VV, Wu SSY, Kume ES, Paulson K, Chan APK *et al*. AMP-activated protein kinase influences metabolic remodeling in H9c2 cells hypertrophied by arginine vasopressin. *Am J Physiol Heart Circ Physiol* 2009; **296**: H1822–H1832.
- 74 Shaw MMM, Reuben J. The AMP-activated protein kinase (AMPK) signaling pathway coordinates cell growth, autophagy, & metabolism. *Nat Cell Biol* 2011; **13**: 1016–1023.
- 75 Kiffin R, Bandyopadhyay U, Cuervo AM. Oxidative stress and autophagy. *Antioxidants Redox Signal* 2006; **8**: 152–162.
- 76 Lemasters JJ. Selective mitochondrial autophagy, or mitophagy, as a targeted defense against oxidative stress, mitochondrial dysfunction, and aging. *Rejuvenation Res* 2005; **8**: 3–5.
- 77 Han J, Pan XY, Xu Y, Xiao Y, An Y, Tie L *et al*. Curcumin induces autophagy to protect vascular endothelial cell survival from oxidative stress damage. *Autophagy* 2012; **8**: 812–825.



This work is licensed under a Creative Commons Attribution-NonCommercial-NoDerivs 4.0 International License. The images or other third party material in this article are included in the article's Creative Commons license, unless indicated otherwise in the credit line; if the material is not included under the Creative Commons license, users will need to obtain permission from the license holder to reproduce the material. To view a copy of this license, visit <http://creativecommons.org/licenses/by-nc-nd/4.0/>

© The Author(s) 2017

Supplementary Information accompanies the paper on the Translational Psychiatry website (<http://www.nature.com/tp>)